



This discussion paper is/has been under review for the journal Geoscientific Model Development (GMD). Please refer to the corresponding final paper in GMD if available.

# Complementing thermosteric sea level rise estimates

K. Lorbacher<sup>1</sup>, M. Meinshausen<sup>1,2</sup>, and A. Nauels<sup>1</sup>

<sup>1</sup>Australian-German College of Climate & Energy Transitions, The University of Melbourne, Parkville 3010, Victoria, Australia

<sup>2</sup>The Potsdam Institute for Climate Impact Research, Telegrafenberg A26, 14412 Potsdam, Germany

Received: 9 December 2014 – Accepted: 23 January 2015 – Published: 10 February 2015

Correspondence to: K. Lorbacher (katja.dommenget@climate-energy-college.org)

Published by Copernicus Publications on behalf of the European Geosciences Union.

GMDD

8, 1201–1223, 2015

## Complementing thslr estimates

K. Lorbacher et al.

[Title Page](#)

[Abstract](#)

[Introduction](#)

[Conclusions](#)

[References](#)

[Tables](#)

[Figures](#)

◀

▶

◀

▶

[Back](#)

[Close](#)

[Full Screen / Esc](#)

[Printer-friendly Version](#)

[Interactive Discussion](#)



## Abstract

Thermal expansion of seawater is one of the most important contributors to global sea level rise in the past 100 years. Yet, observational estimates of thermal expansion are sparse, mostly limited to the upper ocean layers, and only a part of the available climate model data is sufficiently diagnosed to complete our quantitative understanding of thermosteric sea level rise (thSLR). In order to support usage of results of the Coupled Model Intercomparison Project Phase 5 (CMIP5), complement observations and enable the development of surrogate techniques to project thSLR, we complete diagnostics of CMIP5 models. We obtain 30 % more thermal expansion time series than currently published. We find that upper 700 m (2000 m) observational estimates need to be augmented by  $36 \pm 9\%$  ( $15 \pm 6\%$ ) on average to be considered for a global sea level budget. Half of the total expansion originates from depths below  $480 \pm 250$  m – with the range indicating scenario-to-scenario variations. Lastly, to support the development of surrogate methods to project thermal expansion, we calibrate two simplified parameterisations against CMIP5 estimates of thSLR: one parameterisation is suitable for scenarios where only hemispheric ocean temperature profiles are available, the other, where total ocean heat uptake is known (goodness-of-fit:  $\pm 5$  and  $\pm 9\%$ , respectively).

## 1 Introduction

Sea level rise due to anthropogenic climate change constitutes a major impact to the world's coastlines, low-lying deltas and small island states. The climate system is warming and during the relatively well-sampled recent 40 year period (1970–2010) the world ocean stored 30 % of the net heating in depths below 700 m (Rhein et al., 2013). As the ocean takes up heat, the thermal expansion of seawater is a major driver behind sea level rise (SLR). This volumetric response of the ocean to temperature changes, to the uptake and redistribution of heat, is expressed by its thermal expansion coefficient

## Complementing thslr estimates

K. Lorbacher et al.

[Title Page](#)

[Abstract](#)

[Introduction](#)

[Conclusions](#)

[References](#)

[Tables](#)

[Figures](#)

◀

▶

◀

▶

[Back](#)

[Close](#)

[Full Screen / Esc](#)

[Printer-friendly Version](#)

[Interactive Discussion](#)



Complementing thslr estimates

K. Lorbacher et al.

$\alpha$  (e.g., Griffies et al., 2014) and is due to (nonlinearities of) the thermodynamic properties (potential temperature,  $\Theta$ , salinity,  $S$ , and pressure,  $p$ ) in the equation of state of seawater density,  $\rho$  (e.g., Jackett et al., 2006). Thus, changes in heat fluxes at the sea surface and heat redistribution in ocean's interior by advection, eddies and diffusion, lead to non-zero temperature differences altering the sea level even if the global mean potential temperature changes equal zero (Lowe and Gregory, 2006; Piecuch and Ponte, 2014). Sea level is often defined as the height of the sea surface relative to the geoid – the surface of equal gravitational potential of a hypothetical ocean at rest – also called the geocentric sea level according to Church et al. (2013a). Thus sea level changes integrate all volume changes of the world ocean.

Aside from thermal expansion, SLR is also induced by changes in ice-sheets as well as glaciers mass and land water storage. Over the last century these mass changes in the ocean (termed “barystatic” sea level changes by Gregory et al., 2013a) together with ocean's thermal expansion are the main contributors to global mean SLR; some other influences, such as salinity variations associated with freshwater tendencies at the sea surface and redistributed in ocean's interior have a negligible effect on seawater density and thus global mean sea level changes (e.g., Lowe and Gregory, 2006). In the long term, the mass contribution might become substantially larger than thermal expansion contribution to SLR because of the larger efficiency of land-ice melting for a given amount of heat (Trenberth and Fasullo, 2010). However, simulating the land ice-sheet discharge dynamics, for example from the Antarctic Ice Sheets, still translates into large uncertainties in climate models, since irreversible non-linear processes may be triggered that could alter the sea level rise contribution dramatically (e.g., Joughin et al., 2014; Rignot et al., 2014; Mengel and Levermann, 2014). For the observational record with satellite altimeter data since 1993 the observed and simulated contribution of thermosteric expansion to global mean SLR amounts to 34 and 47 %, respectively (see Table 13.1 in Church et al., 2013a). Up to date, the observed contribution to SLR from thermal expansion is limited in space and time dimensions: available observed long-term (decadal) time series of thermosteric sea level rise (thSLR) are mainly globally-

<a href="#">Title Page</a>	
<a href="#">Abstract</a>	<a href="#">Introduction</a>
<a href="#">Conclusions</a>	<a href="#">References</a>
<a href="#">Tables</a> <a href="#">Figures</a>	
<a href="#">◀</a>	<a href="#">▶</a>
<a href="#">◀</a>	<a href="#">▶</a>
<a href="#">Back</a>	<a href="#">Close</a>
<a href="#">Full Screen / Esc</a>	
<a href="#">Printer-friendly Version</a>	
<a href="#">Interactive Discussion</a>	



averaged values using different spatio-temporal interpolation/reconstruction methods and cover the upper 2000 m at maximum (Domingues et al., 2008; Ishii and Kimoto, 2009; Levitus et al., 2012). Observed contributions to thSLR from depths below 2000 m are assumed to increase monotonically and linearly in time (Purkey and Johnson, 2010; Kouketsu et al., 2011).

The objective of the present study is both to complement observed and existing simulated thSLR estimates in a number of ways and to enable the development of surrogate techniques for thSLR projections. We begin by calculating the simulated thermal expansion over the whole ocean depth for a number of CMIP5 models that did not publish those time series yet, after introducing the simulated and observed datasets as well as the method to derive thSLR. Sections 3 and 4 present both the extended CMIP5 thSLR (*zostoga*) dataset and depth-dependent results that can complement upper ocean layer observations. Sections 5 and 6 investigate hemispheric and global averages of calibrated thSLR mimicking CMIP5 estimates. In Sect. 7 we discuss and summarize our results focussing on the extent the observations might underestimate the contribution to thSLR from depths below the main thermocline.

## 2 Methods and models

The volumetric response to changes in ocean's heat budget, the thermosteric sea level,  $\eta_\Theta$ , at any horizontal grid point and any arbitrary time step is defined by the vertically integrated product of the thermal expansion coefficient,  $\alpha$ , and the potential temperature deviation from a reference state,  $\Theta_{\text{exp}} - \Theta_{\text{ref}}$ ,

$$\eta_\Theta(x, y, t) = \int_{-H}^0 \alpha(\Theta_{\text{exp}} - \Theta_{\text{ref}}) dz \quad (1)$$

## Complementing thslr estimates

K. Lorbacher et al.

[Title Page](#)

[Abstract](#)

[Introduction](#)

[Conclusions](#)

[References](#)

[Tables](#)

[Figures](#)

◀

▶

◀

▶

[Back](#)

[Close](#)

[Full Screen / Esc](#)

[Printer-friendly Version](#)

[Interactive Discussion](#)



where the 3-D thermal expansion coefficient,  $\alpha$  is defined by:

$$\alpha = \frac{-1}{\rho(S_{\text{ref}}, \Theta_{\text{ref}}, p)} \frac{\rho(S_{\text{ref}}, \Theta_{\text{exp}}, p) - \rho(S_{\text{ref}}, \Theta_{\text{ref}}, p)}{(\Theta_{\text{exp}} - \Theta_{\text{ref}})} \quad (2)$$

CMIP5 publishes time series of global mean (0-D)  $\eta_{\Theta}$ , called *zostoga* and represents the integral value of ocean's *thermal expansion*,  $\alpha (\Theta_{\text{exp}} - \Theta_{\text{ref}})$ , at each grid point, over the whole ocean volume. For the majority of the fully coupled climate models sea level changes due to net gain of heat need to be diagnosed offline as a result of using the Boussinesq approximation, conserving ocean's volume and not mass (Greatbatch, 1994). Here, we derive global mean yearly depth profiles of thermal expansion by using  $\Theta$  and  $S$  prognostics of CMIP5 model simulations in Eq. (2).

In order to derive thermal expansion estimates, thus *zostoga*, from hemispherically- or globally-averaged vertical temperature profiles, rather than spatial 3-D fields of temperature, salinity and pressure, we use a simplified parameterisation of a thermal expansion coefficient,  $\alpha_{1.5}$ , as a polynomial of  $\Theta$  and  $p$ :

$$\begin{aligned} \alpha_{1.5} = & (c_0 + c_1 \Theta_0 (12.9635 - 1.0833p) - c_2 \Theta_1 (0.1713 - 0.019263p) \\ & + c_3 \Theta_2 (10.41 - 1.1338p) + c_4 p - c_5 p^2) 1.e^{-6}, \end{aligned} \quad (3)$$

with  $\Theta_0 = \Theta_{\text{exp}}$ ,  $\Theta_1 = \Theta_0^2$  and  $\Theta_2 = \Theta_0^3/6000$  and calibration parameters  $c_{n=0-5}$ ; the depth profile,  $z$ , converts into a pressure profile by  $p = 0.0098(0.1005z + 10.5\exp(-1.z/3500) - 1.0)$ . This polynomial algorithm simplifies the equation of state of seawater given in Gill (1982), assuming a constant salinity of 35 psu. It has for example been part of the reduced-complexity Model for the Assessment of Greenhouse Gas Induced Climate Change (MAGICC) (Raper et al., 1996; Wigley et al., 2009; Meinshausen et al., 2011). As a first step, we use for each hemisphere, the time-dependent vertical profiles of  $\Theta$  from the CMIP5 models to calibrate  $\alpha_{1.5}$  by the calibration parameters  $c_n$  against hemispherically-averaged vertical profiles of  $\alpha$  in Eq. (2) (using squared differences as goodness-of-fit statistic).

[Title Page](#)

[Abstract](#)

[Introduction](#)

[Conclusions](#)

[References](#)

[Tables](#)

[Figures](#)

◀

▶

◀

▶

[Back](#)

[Close](#)

[Full Screen / Esc](#)

[Printer-friendly Version](#)

[Interactive Discussion](#)



## Complementing thSLR estimates

K. Lorbacher et al.

[Title Page](#)[Abstract](#)[Introduction](#)[Conclusions](#)[References](#)[Tables](#)[Figures](#)[◀](#)[▶](#)[◀](#)[▶](#)[Back](#)[Close](#)[Full Screen / Esc](#)[Printer-friendly Version](#)[Interactive Discussion](#)

### 3 Extended CMIP5 *zostoga* dataset

For CMIP5 models that report *zostoga*, we calculate the RMS-error between published *zostoga* values and our recalculated values based on the provided  $\Theta$  and initial  $S$  depth profiles. Averaged over all CMIP5 models and scenarios and normalised by the mean 5 *zostoga* value the RMS-error amounts to  $\pm 1\%$ , providing confidence that our 3-D equation of state implementation coincides with those of CMIP5 modelling groups. As not all CMIP5 models that provide  $\Theta$  and  $S$  also provide *zostoga*, our recalculated dataset comprises 30 % more time series of *zostoga* than previously published, available at URL(TBA) (see Table S1 and Fig. 1a).

10 Our extended dataset implies a maximum thSLR of 40 cm thSLR for the 21st century for the RCPs. The model median and its 90 % confidence interval by the mid- and end of the 21st century indicate that previous CMIP5 multi-model ensemble estimates by Church et al. (2013a) have been robust, despite being based on 30 % less models than used here (Tables 1 and S1). The idealised scenarios due to increasing  $\text{CO}_2$  reveal 15 a concave thSLR up to 40 cm in  $1\text{pctCO}_2$  and a convex sea level rise up to 80 cm in *abrupt4xCO<sub>2</sub>* over the first 100 years.

### 4 Complementing observations

Our multi-model ensemble median contribution of thermal expansion to the global mean SLR for the period 1993–2010 is  $1.1 \text{ mm yr}^{-1}$ , with [0.8 to 1.4] as 90 % confidence 20 interval. It reproduces the observational estimates listed in Table 13.1 by Church et al. (2013a). Additionally, this table shows that over this time period the number of available models seems to have an influence on the thSLR: based on 70 % of the dataset used here the simulated trend for 1993–2010 is  $1.49 \text{ mm yr}^{-1}$  [0.97 to 2.02] (cf. Table 13.1 by Church et al., 2013a), thus 13 % higher than both the observational and 25 our estimates. For the upper 700 m, the amplitude of our extended CMIP5 model mean thSLR from 1970s onward amounts to  $0.56 \pm 0.03 \text{ mm yr}^{-1}$  (Fig. 1b) and is very simi-

[Title Page](#)[Abstract](#)[Introduction](#)[Conclusions](#)[References](#)[Tables](#)[Figures](#)[|◀](#)[▶|](#)[◀](#)[▶](#)[Back](#)[Close](#)[Full Screen / Esc](#)[Printer-friendly Version](#)[Interactive Discussion](#)

## Complementing thSLR estimates

K. Lorbacher et al.

[Title Page](#)[Abstract](#)[Introduction](#)[Conclusions](#)[References](#)[Tables](#)[Figures](#)[◀](#)[▶](#)[◀](#)[▶](#)[Back](#)[Close](#)[Full Screen / Esc](#)[Printer-friendly Version](#)[Interactive Discussion](#)

lar to the observed arithmetic mean  $0.54 \pm 0.02 \text{ mm yr}^{-1}$  of the three individual trends  $0.64 \pm 0.02 \text{ mm yr}^{-1}$  (Domingues et al., 2008),  $0.45 \pm 0.02 \text{ mm yr}^{-1}$  (Ishii and Kimoto, 2009) and  $0.52 \pm 0.03 \text{ mm yr}^{-1}$  (Levitus et al., 2012) (cf. Fig. 13.4 in Church et al., 2013a). Around half of the models underestimate ocean's thermal expansion in simulations since the warming period of the upper ocean (above 700 m) commenced in year 5 1971 (Rhein et al., 2013), even after the correction for missing volcanic forcing in the *piControl* scenario (Gregory et al., 2013b). Nevertheless, the majority of the *historical* scenarios capture the main volcanic eruptions in the years 1963 (Agung), 1982 (El Chichon) and 1991 (Pinatubo) with a sea level drop 1–2 years later. Generally, differences

10 in the observed and interannual variability suggest that the underlying spatial pattern of interannual thermosteric sea level variability are different Fyfe et al. (2010).

The model median contribution to thSLR from the layer between 700-to-2000 m suggests a slight underestimation of the observational data (Fig. 1c). For ocean depths below 2000 m, the model median trend for the years 1990–2000 of  $0.11 \text{ mm yr}^{-1}$  in the 15 *historical* scenario seems to reliably represent the contribution to thSLR, which Purkey and Johnson (2010) estimated (Fig. 1d). Based on observed and, by assimilating data, reproduced ocean warming occurring at depth below 3000 m Kouketsu et al. (2011) estimate a similar thSLR over a 40 year period; it amounts to  $0.10$  and  $0.13 \text{ mm yr}^{-1}$ , respectively.

20 The depth profiles of thermodynamic properties across CMIP5 models are largely aligned with observational profiles of potential temperature, salinity by Roemmich and Gilson (2009) and derived thermal expansion coefficient (Fig. 2 and cf. depth profiles of potential temperatures in the *piControl* scenario by Kuhlbrodt and Gregory, 2012). The simulated salinity profile shows the observed maximum around 200 m that reflects evaporation zones and a minimum at around 500 m that reflects mode water regions. 25 For depths below 500 m, the model spread of  $\Theta$  and  $S$  amounts to  $2^\circ\text{C}$  and  $0.4 \text{ psu}$ , respectively. Independent of the model and scenario the global mean thermal expansion coefficient  $\alpha$  shows the familiar concave vertical profile (e.g., Griffies et al., 2014) with a minimum around 1500 m (Fig. 2). The minimum global mean climatological value of

## Complementing thSLR estimates

K. Lorbacher et al.

[Title Page](#)[Abstract](#)[Introduction](#)[Conclusions](#)[References](#)[Tables](#)[Figures](#)[◀](#)[▶](#)[◀](#)[▶](#)[Back](#)[Close](#)[Full Screen / Esc](#)[Printer-friendly Version](#)[Interactive Discussion](#)

$\alpha$  amounts to  $1.3 \times 10^{-4} \text{ }^{\circ}\text{C}^{-1}$  for the *historical* scenario and agrees well with the observed one. Averaged over the whole water column  $\alpha$  ( $1.56 \times 10^{-4} \text{ }^{\circ}\text{C}^{-1}$ ) compares well with the corresponding value from ocean-only simulations ( $1.54 \times 10^{-4} \text{ }^{\circ}\text{C}^{-1}$ , Griffies et al., 2014). In the Northern Hemisphere,  $\alpha$  is 1 % higher than in the Southern Hemisphere because average temperatures tend to be higher above 2000 m in the Northern Hemisphere (not shown). For details in the horizontal and vertical behaviour of  $\alpha$  see e.g. Griffies et al. (2014); Palter et al. (2014).

The median percentage contribution to thSLR from depths below 700 and below 2000 m both clearly depends on the scenario and hence the atmospheric forcing (Fig. 3). The higher the radiative forcing the lower is the contribution from depths below 2000 m and the stronger the warming signal in ocean's upper layers the more enhanced is the stratification in the upper layers, respectively. The exception is the *abrupt4xCO<sub>2</sub>* scenario where the thermal expansion is confined to 90 % in the upper 700 m in the first 20 years. The idealized experiments are started from equilibrium and underestimate the thermal expansion that should have taken place in the real world's post-industrial climate (cf. Russell et al., 2000). Thus the initial extreme warming pulse in *abrupt4xCO<sub>2</sub>* sets up a large vertical temperature gradient between surface and deeper water. Mixing and advection erodes this large vertical temperature gradient that after 90 years the contribution below 700 m increased to 33 % and below 2000 m to 7 %. Because the multi-gas scenarios are not started from equilibrium but from year 2006, the trend of the deeper layers contribution over the 21st century is the reverse: At the beginning of the 21st century, it starts at high levels around 40 % (20 %) for depth below 700 m (2000 m) and then decreases because of the warming induced intensified stratification in the upper 700 m. At the end of the 21st century the projected median and its 90 % confidence interval of the percentage contribution to thSLR from depth below 700 m (and below 2000 m) amount to 33 % [22 to 57%] (and 9 % [2 to 21%]) for the highest emission scenario (*rcp8.5*) and to for the lowest emission scenario (*rcp2.6*) 44 % [31 to 69%] (and 15 % [4 to 36%]). The corresponding values for the historical scenario during the reference period for the emission scenarios (1986–2005, Church



et al., 2013a) are 46 % [21 to 77%] (and 22 % [4 to 46%]). Rhein et al. (2013) note that the observed warming signal of ocean's upper 700 m during 1971 to 2010 seemed to increase the stratification in the upper 200 m by 4 %. During 1971 to 2005 we estimate an increase in the multi-model median contribution to thSLR in the upper 700 m by 8 % (Fig. 3e).

## 5 The 1.5-D parameterisation

Minimising RMS errors, we obtain 6 calibration parameters  $c_n$  for each CMIP5 model. When comparing our extended set of CMIP5 thSLR (*zostoga*) time series with the thSLR time series obtained by using potential temperatures and standard pressure profiles with Eq. (3), we then obtain an average error of  $\pm 5\%$ , ranging in between 1 and 17 % across the CMIP5 model suite (see Table S2). The hemispherically-averaged percentage contributions to thSLR based on the 1.5-D simplified thermal expansion coefficient (Eq. 3) for all seven scenarios compare well with our extended CMIP5 dataset (Fig. 4). The thermal expansion related contribution to SLR from depths below 2000 m is larger in Southern Hemisphere than in Northern Hemisphere and might be due to model dependent mixing rates forming Antarctic bottom water. Strong outliers (values far outside the whiskers and the 90 % confidence interval, respectively) are found in the depth range between 700–2000 m independent of the scenario and spatial averaging, in the depth range of the main thermocline.

## 20 6 The 0-D parameterisation

Our findings complement Kuhlbrodt and Gregory (2012) who analysed the “expansion efficiency of heat”, the constant of proportionality between thSLR and OHU, for the *1pctCO<sub>2</sub>* scenarios and concluded that model differences in the stratification below the main thermocline largely explain the differences between the individual models. Based on the ensemble of 30 %-less CMIP5 models than used here, the constant for

global mean (0-D) time series estimated by Kuhlbrodt and Gregory (2012) amounts to  $0.11 \pm 0.01 \text{ m YJ}^{-1}$ . Our median and its 90 % confidence interval amount to  $0.12 \text{ m YJ}^{-1}$  [0.10 to 0.14] as integral over the whole water depths,  $0.14 \text{ m YJ}^{-1}$  [0.12 to 0.15] for the upper 700 m and  $0.10 \text{ m YJ}^{-1}$  [0.08 to 0.11] below 700 m (Table S3.1). The constant depends on the 3-D-pattern of heat redistribution with the main contribution arising from the upper 700 m. This pattern depends in equal measure on the individual model and on the scenario for a given model (see Tables S3.1 and S3.2).

## 7 Discussion and summary

With observational estimates being primarily available for the upper ocean layers and non-significant contributions to global mean thSLR from depths below 2000 m during 2005 to 2013 (Llovel et al., 2014), our results show that estimates of thSLR for the upper 700 m have to be augmented on average by  $36 \pm 9\%$  (cf. Domingues et al., 2008) and for the upper 2000 m by  $15 \pm 6\%$  to be considered for a global sea level budget. In fact, our results indicate that half of the thSLR contributions comes from depths below 480 m in the *historical* runs and from slightly shallower levels in the future RCP scenarios – averaged across the last 20 years of the scenario period (Fig. 5).

Half of the OHU can be attributed to  $\sim 100$  m deeper layers than of thSLR due to nonlinearities in the seawater equation of state (not shown). Furthermore, our results show that those “half-depths” are deeper in the southern than Northern Hemisphere because the layers above 2000 m are warmer in the Northern Hemisphere and less stratified below the main thermocline than the water masses in the Southern Hemisphere. The recent study by Durack et al. (2014) corroborates the relevance for hemispheric partitioning of model results to adjust for the poor sampling of the Southern Hemisphere’s upper ocean temperature. The depths where the mean of thSLR originates are  $\sim 100\text{--}200$  m below the median-depths (Fig. 5). This indicates a positive skewness of the vertical distribution of thSLR because of its long tail towards depths below 700 m with the exception of the *historical* scenario: For the period 1986–2005 the

## Complementing thslr estimates

K. Lorbacher et al.

[Title Page](#)

[Abstract](#)

[Introduction](#)

[Conclusions](#)

[References](#)

[Tables](#)

[Figures](#)

◀

▶

◀

▶

[Back](#)

[Close](#)

[Full Screen / Esc](#)

[Printer-friendly Version](#)

[Interactive Discussion](#)



amount of thSLR is small compared to the underlying interannual variability because of the internal variability of ocean dynamics. However, all these findings highlight that the contribution to the present and projected thSLR is not predominantly (> 50 %) attributable to the layers above the depth of 700 m, the depth most observational based estimated are still limited to (Domingues et al., 2008; Ishii and Kimoto, 2009; Levitus et al., 2012).

Generally, expanding a mass of warm, salty subtropical water is more efficient for a given temperature increase than a mass of cold, fresh subpolar water for the same temperature increase. In upper tropical waters a warming signal persists longer than in upper high-latitude waters due to the weaker, temperature dominated stratification in higher latitudes, except in the Southern Ocean around Antarctica where salinity changes play a fundamental role in determining the strength of stratification (Bindoff and Hobbs, 2013; Rye et al., 2014). Our diagnosis of CMIP5 profiles confirms the large variations in  $\alpha$  due to strong vertical density gradients (see Fig. 2). These strong vertical as well as meridional gradients in the thermal expansion efficiency raise the question whether simplified approaches that collapse either the meridional component (our 1.5-D simplification) or both dimensions (the 0-D approach) are sufficiently reliable. The introduced errors of  $\pm 5$  and  $\pm 9\%$ , respectively, suggest that the simplifications are sufficiently accurate for long-term SLR projections, when other uncertainties (land ice-sheet response, climate sensitivity or radiative forcing, e.g., Hallberg et al., 2013) tend to dominate the final result.

The Supplement related to this article is available online at  
[doi:10.5194/gmdd-8-1201-2015-supplement](https://doi.org/10.5194/gmdd-8-1201-2015-supplement).

Author contributions. All authors contributed designing and writing the text. K. Lorbacher conducted the analysis and drafted the manuscript.

## Complementing thslr estimates

K. Lorbacher et al.

[Title Page](#)

[Abstract](#)

[Introduction](#)

[Conclusions](#)

[References](#)

[Tables](#)

[Figures](#)

◀

▶

◀

▶

[Back](#)

[Close](#)

[Full Screen / Esc](#)

[Printer-friendly Version](#)

[Interactive Discussion](#)



Complementing thslr estimates

K. Lorbacher et al.

Title Page

Abstract

Introduction

Conclusions

References

Tables

Figures

◀

▶

◀

▶

Back

Close

Full Screen / Esc

Printer-friendly Version

Interactive Discussion



**Acknowledgements.** We thank Dimitri Lafleur for his valuable and helpful comments on the manuscript. We acknowledge the World Climate Research Programme's Working Group on Coupled Modelling, which is responsible for CMIP, and we thank the climate modeling groups (listed in Table S1 of this paper and based on [http://cmip-pcmdi.llnl.gov/cmip5/docs/CMIP5\\_modeling\\_groups.pdf](http://cmip-pcmdi.llnl.gov/cmip5/docs/CMIP5_modeling_groups.pdf)) for producing and making available their model output. For CMIP the U.S. Department of Energy's Program for Climate Model Diagnosis and Intercomparison provides coordinating support and led development of software infrastructure in partnership with the Global Organization for Earth System Science Portals. Observational data by Domingues et al. (2008), Ishii and Kimoto (2009), Levitus et al. (2012) and Roemmich and Gilson (2009) are provided at [http://www.cmar.csiro.au/sealevel/sl\\_data\\_cmar.html](http://www.cmar.csiro.au/sealevel/sl_data_cmar.html), <http://atm-phys.nies.go.jp/~ism/pub/ProjD>, [http://www.nodc.noaa.gov/OC5/3M\\_HEAT\\_CONTENT/basin\\_tsl\\_data.html](http://www.nodc.noaa.gov/OC5/3M_HEAT_CONTENT/basin_tsl_data.html) and [http://sio-argo.ucsd.edu/RG\\_Climatology.html](http://sio-argo.ucsd.edu/RG_Climatology.html), respectively.

## References

- Bindoff, N. L. and Hobbs, W. R.: Oceanography: deep ocean freshening, *Nat. Clim. Change*, 3, 864–865, doi:10.1038/nclimate2014, 2013. 1212
- Church, J. A., Clark, P. U., Cazenave, A., Gregory, J. M., Jevrejeva, S., Levermann, A., Merrifield, M. A., Milne, G. A., Nerem, R. S., Nunn, P. D., Payne, A. J., Pfeffer, W. T., Stammer, D., and Unnikrishnan, A. S.: Sea level change, in: *Climate Change 2013: The Physical Science Basis. Contribution of Working Group I to the Fifth Assessment Report of the Intergovernmental Panel on Climate Change*, edited by: Stocker, T. F., Qin, D., Plattner, G.-K., Tignor, M., Allen, S. K., Boschung, J., Nauels, A., Xia, Y., Bex, V., and Midgley, P. M., Cambridge University Press, Cambridge, UK and New York, NY, USA, 1137–1216, 2013a. 1203, 1207, 1208
- Church, J. A., Monselesan, D., Gregory, J. M., and Marzeion, B.: Evaluating the ability of process based models to project sea-level change, *Environ. Res. Lett.*, 8, 014051, doi:10.1088/1748-9326/8/1/014051, 2013b. 1206
- Domingues, C. M., Church, J. A., White, N. J., Gleckler, P. J., Wijffels, S. E., Barker, P. M., and Dunn, J. R.: Improved estimates of upper-ocean warming and multi-decadal sea level rise, *Nature*, 453, 1090–1093, doi:10.1038/nature07080, 2008. 1204, 1208, 1211, 1212, 1213, 1219

## Complementing thslr estimates

K. Lorbacher et al.

[Title Page](#)

[Abstract](#)

[Introduction](#)

[Conclusions](#)

[References](#)

[Tables](#)

[Figures](#)

◀

▶

◀

▶

[Back](#)

[Close](#)

[Full Screen / Esc](#)

[Printer-friendly Version](#)

[Interactive Discussion](#)



Durack, P. J., Gleckler, P. J., Landerer, F. W., and Taylor, K. E.: Quantifying underestimates of long-term upper-ocean warming, *Nat. Clim. Change*, 4, 999–1005, doi:10.1038/nclimate2389, 2014. 1211

Fyfe, J. C., Gillett, N. P., and Thompson, D. W. J.: Comparing variability and trends in observed and modelled global-mean surface temperature, *Geophys. Res. Lett.*, 37, L16802, doi:10.1029/2010GL044255, 2010. 1208

Gill, A. E.: *Atmosphere-Ocean Dynamics*, Academic Press, San Diego, California, USA, 662 pp., 1982. 1205

Greatbatch, R. J.: A note on the representation of steric sea level in models that conserve volume rather than mass, *J. Geophys. Res.*, 99, 12767–12771, 1994. 1205

Gregory, J. M., White, N. J., Church, J. A., Bierkens, M. F. P., Box, J. E., van den Broeke, M. R., Cogley, J. G., Fettweis, X., Hanna, E., Huybrechts, P., Konikow, L. F., Leclercq, P. W., Marzeion, B., Oerlemans, J., Tamisiea, M. E., Wada, Y., Wake, L. M., and van de Wal, R. S. W.: Twentieth-century global-mean sea level rise: is the whole greater than the sum of the parts?, *J. Climate*, 26, 4476–4499, doi:10.1175/JCLI-D-12-00319.1, 2013a. 1203

Gregory, J. M., Bi, D., Collier, M. A., Dix, M. R., Hirst, A. C., Hu, A., Huber, M., Knutti, R., Marsland, S. J., Meinshausen, M., Rashid, H. A., Rotstayn, L. D., Schurer, A., and Church, J. A.: Climate models without volcanic preindustrial volcanic forcing underestimate historical ocean thermal expansion, *Geophys. Res. Lett.*, 40, 1600–1604, doi:10.1002/grl.50339, 2013b. 1206, 1208

Griffies, S. M., Yin, J., Durack, P. J., Goddard, P., Bates, S. C., Behrens, E., Bentsen, M., Bi, D., Biastoch, A., Böning, C. W., Bozec, A., Chassignet, E., Danabasoglu, G., Danilov, S., Domingues, C., Drange, H., Farneti, R., Fernandez, E., Greatbatch, R. J., Holland, D. M., Ilicak, M., Large, W., Lorbacher, K., Lu, J., Marsland, S. J., Mishra, A., Nurser, A. J. G., Salas y Mélia, D., Palter, J. B., Samuels, B. L., Schröter, J., Schwarzkopf, F. U., Sidorenko, D., Treguier, A.-M., Tseng, Y., Tsujino, H., Uotila, P., Valcke, S., Volodire, A., Wang, Q., Winton, M., and Zhang, X.: An assessment of global and regional sea level for years 1993–2007 in a suite of interannual CORE-II simulations, *Ocean Model.*, 78, 35–89, doi:10.1016/j.ocemod.2014.03.004, 2014. 1203, 1208, 1209

Hallberg, R., Adcroft, A., Dunne, J. P., Krasting, J. P., and Stouffer, R. J.: Sensitivity of twenty-first-century global-mean steric sea level rise to ocean model formulation, *J. Climate*, 26, 2947–2956, doi:10.1175/JCLI-D-12-00506.1, 2013. 1212

Complementing thslr estimates

K. Lorbacher et al.

- Ishii, M. and Kimoto, M.: Reevaluation of historical ocean heat content variations with an XBT depth bias correction, *J. Oceanogr.*, 65, 287299, doi:10.1007/s10872-009-0027-7, 2009. 1204, 1208, 1212, 1213, 1219
- Jackett, D. R., McDougall, T. J., Feistel, R., Wright, D. G., and Griffies, S. M.: Algorithms for density, potential temperature, conservative temperature, and the freezing temperature of seawater, *J. Atmos. Ocean. Tech.*, 23, 1709–1728, doi:10.1175/JTECH1946.1, 2006. 1203
- Joughin, I., Smith, B. E., and Medley, B.: Marine ice sheet collapse potentially under way from the Thwaites glacier basin, *Science*, 344, 735–738, doi:10.1126/science.1249055, 2014. 1203
- Kouketsu, S., Doi, T., Kawano, T., Masuda, S., Sugiura, N., Sasaki, Y., Toyoda, T., Igarashi, H., Kawai, Y., Katsumata, K., Uchida, H., Fukasawa, M., and Awaji, T.: Deep ocean heat content changes estimated from observations and reanalysis product and their influence on sea level change, *J. Geophys. Res.*, 116, C03012, doi:10.1029/2010JC006464, 2011. 1204, 1208
- Kuhlbrodt, T. and Gregory, J. M.: Ocean heat uptake and its consequences for the magnitude of sea level rise and climate change, *Geophys. Res. Lett.*, 39, L18608, doi:10.1029/2012GL052952, 2012. 1206, 1208, 1210, 1211
- Levitus, S., Antonov, J. I., Boyer, T. P., Baranova, O. K., Garcia, H. E., Locarnini, R. A., Mishonov, A. V., Reagan, J. R., Seidov, D., Yarosh, E. S., and Zweng, M. M.: World ocean heat content and thermosteric sea level change (0–2000 m), 1955–2010, *Geophys. Res. Lett.*, 39, L10603, doi:10.1029/2012GL051106, 2012. 1204, 1208, 1212, 1213, 1219
- Lowe, J. A. and Gregory, J. M.: Understanding projections of sea level rise in a Hadley Centre coupled climate model, *J. Geophys. Res.*, 111, C11014, doi:10.1029/2005JC003421, 2006. 1203
- Llovel, W., Willis, J. K., Landerer, F. W., and Fukumori, I.: Deep-ocean contribution to sea level and energy budget not detectable over the past decade, *Nat. Clim. Change*, 4, 1031–1035, doi:10.1038/nclimate2387, 2014. 1211
- Meinshausen, M., Raper, S. C. B., and Wigley, T. M. L.: Emulating coupled atmosphere-ocean and carbon cycle models with a simpler model, MAGICC6 2013 Part 1: Model description and calibration, *Atmos. Chem. Phys.*, 11, 1417–1456, doi:10.5194/acp-11-1417-2011, 2011. 1205
- Mengel, M. and Levermann, A.: Ice plug prevents irreversible discharge from East Antarctica, *Nat. Clim. Change*, 4, 451–455, doi:10.1038/nclimate2226, 2014. 1203

<a href="#">Title Page</a>	<a href="#">Abstract</a>	<a href="#">Introduction</a>
<a href="#">Conclusions</a>	<a href="#">References</a>	
<a href="#">Tables</a>	<a href="#">Figures</a>	
<a href="#">◀</a>	<a href="#">▶</a>	
<a href="#">◀</a>	<a href="#">▶</a>	
<a href="#">Back</a>	<a href="#">Close</a>	
<a href="#">Full Screen / Esc</a>		
	<a href="#">Printer-friendly Version</a>	
	<a href="#">Interactive Discussion</a>	



## Complementing thslr estimates

K. Lorbacher et al.

- Moss, R. H., Edmonds, J. A., Hibbard, K. A., Manning, M. R., Rose, S. K., van Vuuren, D. P., Carter, T. R., Emori, S., Kainuma, M., Kram, T., Meehl, G. A., Mitchell, J. F., Nakicenovic, N., Riahi, K., Smith, S. J., Stouffer, R. J., Thomson, A. W., Weyant, J. P., and Wilbanks, T. J.: The next generation of scenarios for climate change research and assessment, *Nature*, 463, 747–756, doi:10.1038/nature08823, 2010. 1206
- Palter, J. B., Griffies, S. M., Samuels, B. L., Galbraith, E. D., Gnanadesikan, A., and Klocker, A.: The deep ocean buoyancy budget and its temporal variability, *J. Climate*, 27, 551–573, doi:10.1175/JCLI-D-13-00016.1, 2014. 1209
- Piecuch, C. G. and Ponte, R. M.: Mechanisms of global-mean steric sea level change, *J. Climate*, 27, 824–834, doi:10.1175/JCLI-D-13-00373.1, 2014. 1203
- Purkey, S. and Johnson, G. C.: Warming of global abyssal and deep southern ocean waters between the 1990s and 2000s: contributions to global heat and sea level rise budgets, *J. Climate*, 3, 6336–6351, doi:10.1175/2010JCLI3682.1, 2010. 1204, 1208, 1219
- Raper, S. C. B., Wigley, T. M. L., and Warrick, R. A.: Global sea-level rise: past and future, in: *Sea-Level Rise and Coastal Subsidence: Causes, Consequences and Strategies*, edited by: Milliman, J. and Haq, B., Kluwer, Dordrecht, the Netherlands, 11–45, 1996. 1205
- Rhein, M., Rintoul, S. R., Aoki, S., Campos, E., Chambers, D., Feely, R. A., Gulev, S., Johnson, G. C., Josey, S. A., Kostianoy, A., Mauritzen, C., Roemmich, D., Talley, L. D., and Wang, F.: Observations: ocean, in: *Climate Change 2013: The Physical Science Basis, Contribution of Working Group I to the Fifth Assessment Report of the Intergovernmental Panel on Climate Change*, edited by: Stocker, T. F., Qin, D., Plattner, G.-K., Tignor, M., Allen, S. K., Boschung, J., Nauels, A., Xia, Y., Bex, V., and Midgley, P. M., Cambridge University Press, Cambridge, UK and New York, NY, USA, 2013. 1202, 1208, 1210
- Rignot, E., Mouginot, J., Morlighem, M., Seroussi, H., and Scheuchl, B.: Widespread rapid grounding line retreat of Pine Island, Thwaites, Smith and Kohler glaciers, West Antarctica from 1992 to 2011, *Geophys. Res. Lett.*, 41, 3502–3509, doi:10.1002/2014GL060140, 2014. 1203
- Roemmich, D. and Gilson, J.: The 2004–2008 mean and annual cycle of temperature, salinity, and steric height in the global ocean from the Argo Program, *Prog. Oceanogr.*, 82, 81–100, doi:10.1029/2011GL047992, 2009. 1208, 1213, 1219
- Rye, C. D., Naveira Garabato, A. C., Holland, P. R., Meredith, M. P., Nurser, A. J., Hughes, C. W., Coward, A. C., and Webb, D.: Rapid sea-level rise along the Antarctic margins in response to increased glacial discharge, *Nat. Geosci.*, 7, 732–735, doi:10.1038/ngeo2230, 2014. 1212

[Title Page](#)[Abstract](#)[Introduction](#)[Conclusions](#)[References](#)[Tables](#)[Figures](#)[◀](#)[▶](#)[◀](#)[▶](#)[Back](#)[Close](#)[Full Screen / Esc](#)[Printer-friendly Version](#)[Interactive Discussion](#)

- Russell, G. L., Gornitz, V., and Miller, J. R.: Regional sea level changes projected by the NASA/GISS atmosphere ocean model, *Clim. Dynam.*, 16, 789–797, 2000. 1206, 1209
- Taylor, K. E., Stouffer, R. J., and Meehl, G. A.: An overview of CMIP5 and the scenario design, *B. Am. Meteorol. Soc.*, 93, 485–498, doi:10.1175/BAMS-D-11-00094.1, 2012. 1206
- 5 Trenberth, K. E. and Fasullo, J. T.: Tracking Earth's energy, *Science*, 328, 316–317, doi:10.1126/science.1187272, 2010. 1203
- Wigley, T. M. L., Clarke, L. E., Edmonds, J. A., Jacoby, H. D., Paltsev, S., Pitcher, H., Reilly, J. M., Richels, R., Sarofim, M. C., and Smith, S. J.: Uncertainties in climate stabilization, *Climatic Change*, 97, 85–121, doi:10.1007/s10584-009-9585-3, 2009. 1205
- 10 Yin, J.: Century to multi-century sea level rise projections from CMIP5 models, *Geophys. Res. Lett.*, 39, L17709, doi:10.1029/2012GL052947, 2012. 1206

## Complementing thslr estimates

K. Lorbacher et al.

[Title Page](#)

[Abstract](#)

[Introduction](#)

[Conclusions](#)

[References](#)

[Tables](#)

[Figures](#)

◀

▶

◀

▶

[Back](#)

[Close](#)

[Full Screen / Esc](#)

[Printer-friendly Version](#)

[Interactive Discussion](#)



## Complementing thSLR estimates

K. Lorbacher et al.

**Table 1.** Median and its 90 % confidence interval for projections of global mean (0-D) thSLR (in m) in 2046–2065 and 2081–2100 relative to 1986–2005 for the four RCP scenarios.

period scenario	1986–2005	2046–2065	2081–2100	2100	2081–2100 IPCC-AR5
historical	0.03 [0.01 to 0.07]				
rcp2.6		0.10 [0.07 to 0.13]	0.14 [0.10 to 0.18]	0.15 [0.10 to 0.20]	0.14 [0.10 to 0.18]
rcp4.5		0.11 [0.08 to 0.14]	0.19 [0.14 to 0.22]	0.21 [0.15 to 0.26]	0.19 [0.14 to 0.23]
rcp6.0		0.10 [0.08 to 0.13]	0.20 [0.15 to 0.24]	0.23 [0.17 to 0.27]	0.19 [0.15 to 0.24]
rcp8.5		0.13 [0.16 to 0.17]	0.27 [0.21 to 0.32]	0.32 [0.25 to 0.39]	0.27 [0.21 to 0.33]

- [Title Page](#)
- [Abstract](#) [Introduction](#)
- [Conclusions](#) [References](#)
- [Tables](#) [Figures](#)
- [◀](#) [▶](#)
- [◀](#) [▶](#)
- [Back](#) [Close](#)
- [Full Screen / Esc](#)
- [Printer-friendly Version](#)
- [Interactive Discussion](#)



## Complementing thSLR estimates

K. Lorbacher et al.

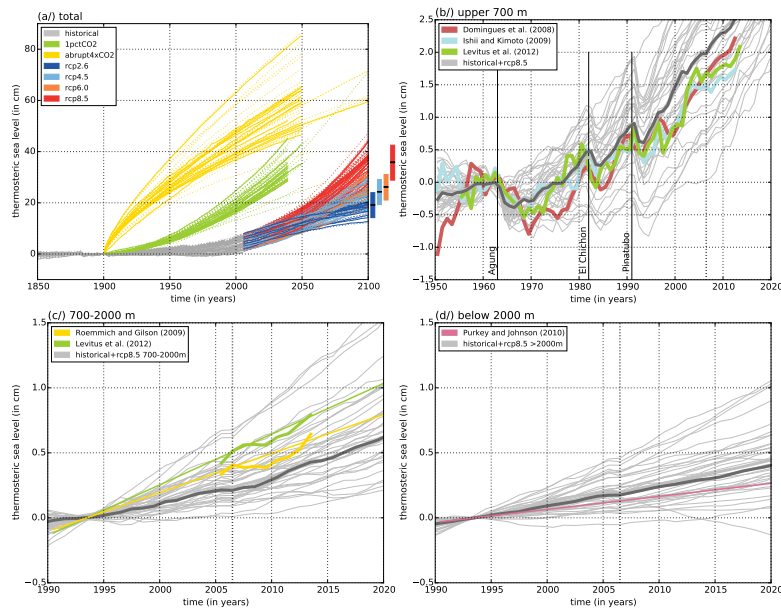


**Figure 1.** Time series of observed and simulated global mean yearly sea level. **(a)** Simulated thermosteric sea level (*zostoga*, in cm) relative to year 1990 for seven CMIP5 scenarios: *historical* (31/47), *1pctCO<sub>2</sub>* (19/32), *abrupt4xCO<sub>2</sub>* (17/30), *rcp2.6* (18/26), *rcp4.5* (27/40), *rcp6.0* (13/20), *rcp8.5* (27/40); the ratio in brackets indicates the number of models of published (solid lines) *zostoga* and recalculated (dashed lines) *zostoga* in this study based on simulated temperature and salinity fields. Bars indicate the thSLR of the four RCP-scenarios in year 2100 relative to year 1900 (see also Table 1). **(b)** Observed contribution to yearly thermosteric sea level (in cm) of the upper 700 m by Domingues et al. (2008); Ishii and Kimoto (2009); Levitus et al. (2012) relative to year 1961 and corresponding simulated time series of the *historical* and *rcp8.5* scenarios, whereby the solid light (dark) grey lines represent the model mean (median). Observed contribution to yearly thermosteric sea level (in cm) from layers **(c)** between 700–2000 m by Levitus et al. (2012); Roemmich and Gilson (2009) and **(d)** below 2000 m by Purkey and Johnson (2010). Corresponding simulated time series are indicated as in **(b)**.

## Complementing thsir estimates

K. Lorbacher et al.

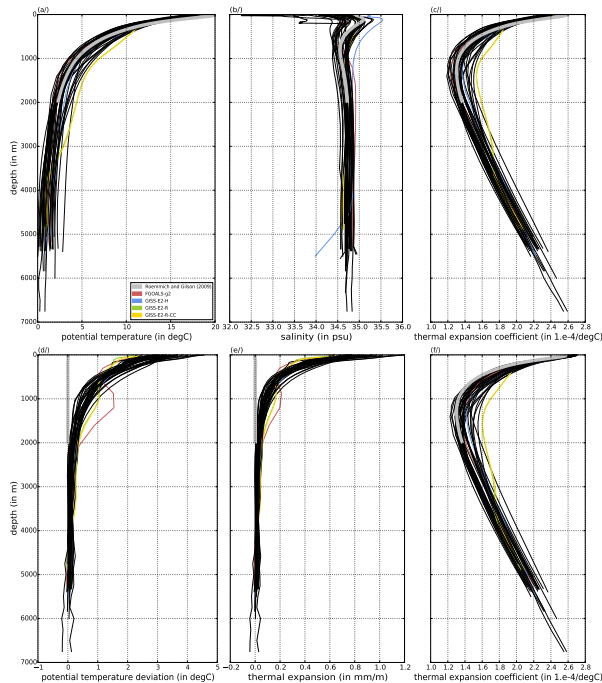


**Figure 2.** Global mean vertical profiles for all models of *historical* in year 1900 (upper panels, **a–c**) and of *rcp8.5* in year 2100 (lower panels, **d–f**): **(a)** potential temperature (in  $^{\circ}\text{C}$ , 0 to 20), **(b)** salinity (in psu, 32 to 36) and **(c)** thermal expansion coefficient  $\alpha$  (in  $10^{-4} \text{ }^{\circ}\text{C}^{-1}$ , 1.2 to 2.8); **(d)** temperature deviation (in  $^{\circ}\text{C}$ , -1 to 5), **(e)** thermal expansion per layer (in  $\text{mm m}^{-1}$ , -0.2 to 1.2) and **(f)** thermal expansion coefficient  $\alpha$  (in  $10^{-4} \text{ }^{\circ}\text{C}^{-1}$ , 1.2 to 2.8). Observed profiles (grey lines) are based on the Argo-data as an average over the period 2005 to 2013, except for the temperature deviation in **(d)** and corresponding thermal expansion in **(e)**. Model outliers are indicated in **(a)**.

## Complementing thSLR estimates

K. Lorbacher et al.

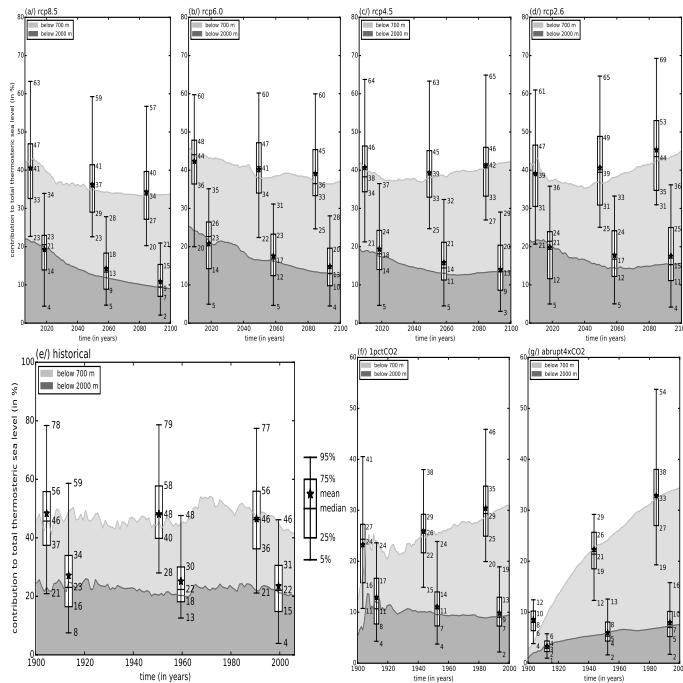


**Figure 3.** Model median percentage contribution to global mean thSLR for the whole water column from depths below 700 m (light grey) and below 2000 m (dark grey) for the *historical* scenario, for projections for the four RCP scenarios and the two idealized CO<sub>2</sub> scenarios derived from Eq. (2). Whisker plots quantify the temporal average distribution of the contribution to thSLR of the first 20 years, the entire time series and the last 20 years, respectively: 2006–2025/2006–2100/2006–2081 for RCPs **(a)–(d)**; 1901–1920/1900–2005/1981–2005 for the *historical* scenario **(e)**; and 1–20/1–100/81–100 for the *1pctCO<sub>2</sub>* and *abrupt4xCO* scenarios **(f)**, **(g)**. Bars and whiskers represent the 25–75 and 5–95 % uncertainties of the median, respectively; the central mark of the bar indicates the model median, the asterisk the model mean.

Complementing *thsLR* estimates

K. Lorbacher et al.

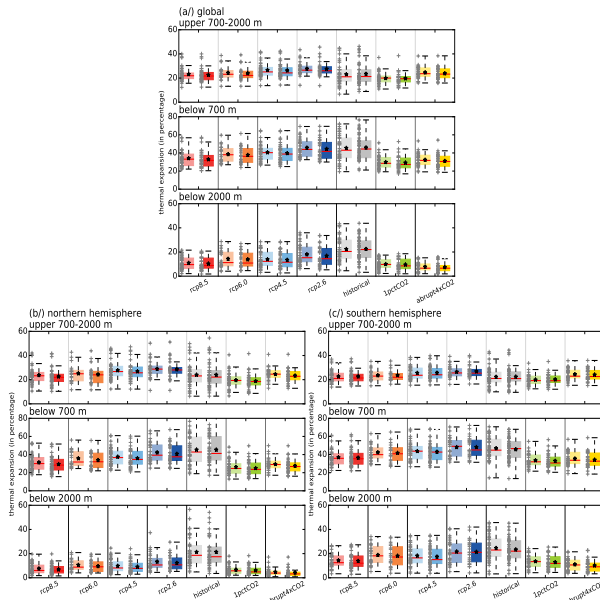


**Figure 4.** Whisker plots of percentage thermal expansion from the layers between 700–2000 m, below 700 and below 2000 m, respectively, relative to the total thermal expansion integrated over the whole water column, for seven scenarios. Thermal expansion estimates are derived from Eq. (2) (left bar) and Eq. (3) (right bar) used in simpler climate models (here with the optimized calibration parameters in Table S2) and based on **(a)** globally, **(b)** northern and **(c)** southern hemispherically-averaged vertical potential temperature profiles, followed by a temporal averaging over the entire time series (see Fig. 3). Bars and whiskers represent the 25–75 and 5–95 % uncertainties of the median, respectively; the central mark of the bar indicates the model median, the asterisk the model mean. The number of models available for these statistical estimates are crosses on the left of the box, at which crosses above and below the whiskers indicate model outliers.

## Discussion Paper | Complementing thSLR estimates

K. Lorbacher et al.

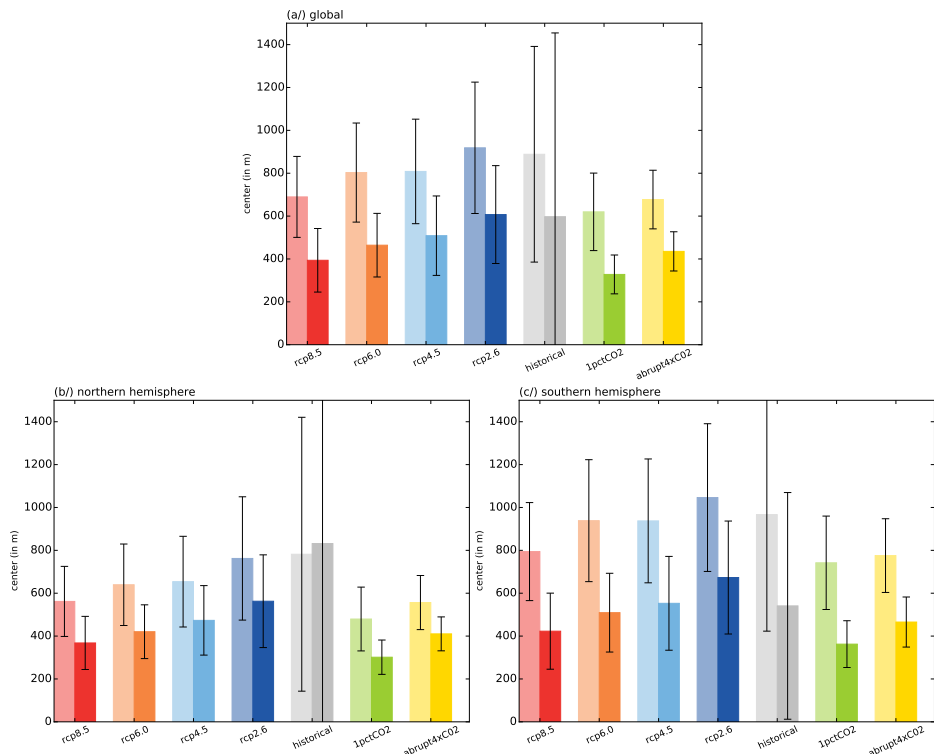


**Figure 5.** Depth and SD (in m) where the multi-model ensemble mean (left bar) and median (right bar) of thSLR originates for the four RCP scenarios, as well as the historical scenario and the two idealized CO<sub>2</sub>-forcing scenarios. Thermal expansion estimates are derived from Eq. (2) based on (a) globally, (b) northern and (c) southern hemispherically-averaged vertical potential temperature profiles, followed by a temporal averaging over the last twenty years (see Figs. 3 and 4). Table S4 summarizes the estimates.